Desalination and Water Treatment
www.deswater.com

doi: 10.1080/19443994.2015.1065442

57 (2016) 13357–13365
June

Taylor & Francis
Taylor & Francis Group

Optimization of Remazol Brilliant Blue adsorption process from aqueous solutions using multi-walled carbon nanotube

A. Arab Markadeh[a], A. Rezaee[b,*], S.O. Rastegar[a], H. Hossini[b], S. Ahmadi[c], E. Hoseinzadeh[b]

[a]*Biotechnology Group, Chemical Engineering Department, Tarbiat Modares University, Tehran, Iran, Tel. +98 2182883980; Fax: +98 2182883517; emails: arash.arab110@gmail.com (A. Arab Markadeh), so.rastegar@gmail.com (S.O. Rastegar)*
[b]*Faculty of Medical Sciences, Department of Environmental Health, Tarbiat Modares University, Tehran, Iran, Tel. +98 2182883590; Fax: +98 2182884555; emails: rezaee@modares.ac.ir (A. Rezaee), hoo.hosseini@gmail.com (H. Hossini), e.hoseinzadeh@modares.ac.ir (E. Hoseinzadeh)*
[c]*Chemical Engineering Department, Tarbiat Modares University, Tehran, Iran, Tel. +98 2182883980; Fax: +98 2182883517; email: saeb.ahmadi@gmail.com*

Received 12 December 2014; Accepted 26 May 2015

ABSTRACT

This work aimed to determine the optimum conditions in order to reach the maximum remazol brilliant blue (RBB) removal and maximum adsorption capacity (uptake) in the sorption process from aqueous solution using multi-walled carbon nanotube (MWCNT). Three factors including initial RBB concentration, initial pH, and initial amount of MWCNTs were optimized using response surface methodology at equilibrium time 15 min. Optimized conditions were RBB concentration 8×10^{-2} mmol/L, initial pH 4.3, and 250-mg MWCNTs. The maximum values for the RBB removal and uptake were 69.06% and 1.1×10^{-2} mM/g, respectively. Among the three used isotherm models including Langmuir, Freundlich and Temkin, the Langmuir isotherm was best fitted with the experimental data because of its higher coefficient value $R^2 = 0.99$.

Keywords: Remazol Brilliant Blue; MWCNT; Response surface methodology; Isotherm

1. Introduction

Dyes contain toxic chemicals that are carcinogenic, mutagenic, or teratogenic [1]. It is now a well-established fact that the coloration of water is mainly caused by dyes, which are generally toxic, non-degradable, and stable [2]. Dye compounds can exist in the effluents from different industries, i.e. textiles, paper, leather, plastics industries, etc., that can penetrate into lakes, rivers, lagoons, and thus inhibiting the biological processes based on photosynthesis [3,4]. It is guesstimated that every year more than 150 thousand tons of different types of dyes are released by these industries into water [2].

Remazol brilliant blue (RBB) is one of the most important pollutant in the textile industry wastewater [5]. RBB represents an important class of often toxic and recalcitrant organopollutants. These dyes contain chromosphore groups. They have the favorable characteristics of bright color, simple application techniques, low energy consumption dyeing process, and high solubility in water [5–7]. Based on the

*Corresponding author.

chromosphore characteristics of dyes, azo is one of the main important groups and the largest class in dyes, comprising around 70% [8]. Indeed, azo dyes with aromatic rings are very complex and are included in the biorecalcitrant class of synthetic compounds [9]. Hence, the wastewater containing dyes must be treated prior to its discharge from the industry. Using different wastewater treatment procedures, the stability of dyes toward light and oxidizing agents also create a problem for their removal. Hence, their removal methods are selected with a great deal of care and thoughtfulness [10]. There are many applied techniques for the treatment of color-contaminated wastewater including adsorption, conventional/advance oxidation, and biological processes [11–14].

It is now well established that adsorption is a much better process than other physical techniques due to its economy and efficacy. Additionally, the ability of adsorption in comparison to biochemical, electrochemical, or photochemical degradation processes to leave behind any toxic degraded products or removing toxic chemicals without disturbing the quality of water has augmented its usage [15,16].

Carbon nanotubes (CNTs) are a new adsorbent material in the carbon family and have been studied intensively for the adsorption of various pollutants from the aqueous matrix [17]. MWCNTs can be classified as concentric and closed graphite tubules with multiple layers of graphite sheets [18]. Due to their unique characteristics such as large surface area and small, hollow and layered structures, the CNT has already been investigated as a promising adsorbent for various organic and inorganic pollutants 19].

In the adsorption process, many factors have been effective, and to optimize them, a method is required. In recent years, response surface methodology (RSM) is being applied successfully in many scientific fields such as biology, chemistry, medicine, and economy [20]. The RSM is based on an experimental design with the final goal of evaluating optimal functioning of industrial facilities, using minimum experimental effort [20]. In this study, determination of effective parameters and region of them including initial RBB concentration, initial pH, and amount of MWCNTs were determined using the RSM that has not been reported by any researcher.

2. Materials and methods

2.1. Materials preparation

The RBB was prepared from DyStar (Germany). The RBB ($C_{22}H_{16}O_{11}N_2S_3Na_2$) belongs to azo group dyes and its molecular weight is 626.5 g/mol. The dye contains NH and SO_3 functional groups as shown in Fig. 1.

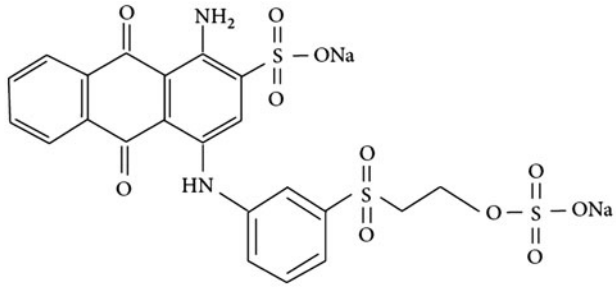

Fig. 1. Structure of the Remazol Brilliant Blue dye.

The maximum adsorption wavelength (λ_{max}) for this was observed at 592 nm. The analysis of RBB was carried out with the calibration method according to optical adsorption by a UV–vis spectrophotometer (Optizen 3220UV, Korea). MWCNTs were purchased from the US Research Nanomaterial Company and its surface area is more than 200 m^2/g.

2.2. Adsorption experiments

The pH was adjusted to the desired value with 1-M HCl and 1-M NaOH. A thermostatic shaker was used to increase the contact between the adsorbent and dye matrix with a 100 rpm for different contact times (0–60 min) and also to control the temperature at 23 ± 2 °C.

2.3. Isotherm models

RBB adsorption data were analyzed using the Langmuir, Freundlich and Temkin isotherms. Langmuir is valid for monolayer adsorption onto a surface containing a finite number of identical sorption sites [21,22]. For the convenience of plotting and determining the Langmuir constants, the linear form given below can be used:

$$\frac{C_e}{q_e} = \frac{1}{K_L q_m} + \frac{C_e}{q_m} \quad (1)$$

Here, q_e is the amount of RBB adsorbed per specific amount of adsorbent in terms of mg/g, C_e is the equilibrium concentration in the solution in terms of mg/L, and q_m is the maximum amount of RBB required to form a monolayer in terms of mg/g. The Langmuir constant, K_L, and monolayer sorption capacity, q_m, were calculated from the slope and the interception of the plot of C_e/q_e and C_e.

Freundlich sorption on a heterogeneous surface is purely empirical [22]. The linearized Freundlich equation in the logarithmic form is given below:

$$\log\ q_e = \log(K_F) + \frac{1}{n}\log(C_e) \tag{2}$$

where K_F and $(1/n)$ represent the equilibrium constant and adsorption intensity, respectively. Values of n between 1 and 10 (i.e. $1/n$ less than 1) represent a favorable adsorption. Equilibrium constants were evaluated from the interception and the slope of the linear plot of ln q_e vs. ln C_e.

Another isotherm which is of investigating importance is the Temkin isotherm. Its linearized form is given below:

$$q_e = B\ \ln(k_t) + B\ \ln(C_e) \tag{3}$$

where $B = RT/b$, b is the Temkin constant related to the heat of sorption (J/mol), k_t is the Temkin isotherm constant (l/g), R is the gas constant (8.314 J/mol K), and T is the absolute temperature (K).

2.4. Response surface methodology

The use of RSM offers an empirical relationship between the response function and the independent variables [23], and the coefficients of the response functions for different dependent variables are determined by correlating the experimental results with the response functions using a Design-Expert regression program.

In the first stage, we found out that the responses function properly with the independent variables. This approximate function must be the polynomial of the independent variables.

$$Y = \beta_i + \sum_{i=1}^{k}\beta_1 x_1 + \sum_{i=1}^{k}\beta_{ii}x_i^2 + \sum_{i=1}^{k}\sum_{j=1}^{k}\beta_{ij}x_i x_j + \varepsilon \tag{4}$$

where Y is the response, β_i, β_1, β_{ii}, and β_{ij} are the coefficients of regression, ε is the error value of the system, and x_j is the coded variable.

The least squares method was used to estimate polynomial approximation. The central composite design (CCD) was used to introduce this model as the most famous design. The CCD levels of the main parameters (RBB concentration, initial pH, and MWCNTs dose) are considered in the form of $-\alpha$, −1, 0, +1, and $+\alpha$. The alpha (significance level) was equal to 1.68. The values for initial RBB were 8×10^{-3}, 4×10^{-2}, 8×10^{-2}, 1.3×10^{-1}, and 1.6×10^{-1} mmol/L, intitail pH were 3.5, 4.3, 5.5, 6.7, and 7.5, and MWCNTs dose was 50, 100, 175, 250, and 300 mg.

3. Results and discussion

3.1. Effect of contact time

The contact time should be considered as an important factor for the interactions between the pollutant and adsorbent. To determine the equilibrium time, 200-mg MWCNTs was added to five levels of dye concentrations (8×10^{-3}, 4×10^{-2}, 8×10^{-2}, 1.3×10^{-1}, and 1.6×10^{-1} mM). This process was limited to a period of 15 min. Accordingly, rapid adsorption of RBB was observed in the first 5 min; next, the adsorption rate decreased gradually and the adsorption reached equilibrium in about 15 min for each concentration and this time was selected as the equilibrium time. The removal percentages were 85, 77.5, 76.25, 70, and 48.75% for the initial concentrations of 8×10^{-3}, 4×10^{-2}, 8×10^{-2}, 1.3×10^{-1}, and 1.6×10^{-1} mM, respectively, in the equilibrium time. The difference in the result demonstrates that the dye adsorption is dependent of the initial concentration. However, this can affect the overall removal percentage and maximum adsorption capacity.

3.2. Statistical analysis

Optimization of three effective factors was done at the equilibrium time of 15 min. RSM designed 20 runs that were showed in Table 1. The ANOVA for RBB adsorption onto MWCNTs is exhibited in Table 2. Values of "Prob > F" less than 0.05 indicate that the models are significant [24].

The second-order (polynomial) regression in terms of coded factors for quadratic model is represented by the following equations:

$$\begin{aligned}\text{RBB removal}\ (\%) = {} & 49.68 - 10.43A - 3.25B + 14.16C \\ & + 1.42AB - 2.10AC - 0.43BC \\ & - 4.23A^2 - 0.84B^2 - 2.13C^2\end{aligned} \tag{5}$$

$$\begin{aligned}\text{Uptake}\ (\text{mmol/L}) = {} & +0.011 + 2.719\text{E}{-}003A \\ & - 7.178\text{E}{-}004B - 9.652\text{E}{-}004C \\ & - 1.054\text{E}{-}004AB - 2.580\text{E}{-}004AC \\ & + 1.986\text{E}{-}004BC - 1.746\text{E}{-}003A^2 \\ & - 2.781\text{E}{-}005B^2 - 2.945\text{E}{-}004C^2\end{aligned} \tag{6}$$

Table 1
The CCD using the nature and coded factors

Run	Initial RBB conc. (mM/L)	Initial pH	Mass of adsorbent (mg)	Experimental	
				RBB removal (%)	Uptake (mM/g)
1	0.085	5.5	175	53	0.0112
2	0.085	5.5	175	50	0.0109
3	0.085	7.5	175	45.5	0.0104
4	0.085	5.5	175	52	0.011
5	0.04	4.3	250	70.4	0.0056
6	0.085	5.5	175	51	0.012
7	0.04	6.6	100	34.4	0.0068
8	0.085	5.5	300	78.12	0.0104
9	0.04	6.6	250	59.8	0.0048
10	0.01	5.5	175	54.88	0.0015
11	0.16	5.5	175	24.67	0.0113
12	0.085	5.5	175	47.4	0.0108
13	0.13	4.3	100	22.7	0.0146
14	0.085	3.5	175	53.22	0.0121
15	0.13	6.6	250	34.6	0.0090
16	0.085	5.5	175	51.24	0.0117
17	0.085	5.5	50	13.3	0.0106
18	0.13	6.6	100	19.5	0.0126
19	0.13	4.3	250	41.4	0.0108
20	0.04	4.3	100	45.2	0.0089

Table 2
ANOVA for response surface quadratic model for RBB adsorption using MWCNTs

	Source	SS	df	MS	*F*-value	*p*-value	
Decolorization (%)	Model	4,602.15	9	511.35	9.2	0.0069	Significant
	A-RBB conc.	1,484.95	1	1,484.95	26.7	0.0021	
	B-initial pH	144.24	1	144.24	2.6	0.1583	
	C-dosage	2,739.2	1	2,739.2	49.3	0.0004	
	AB	16.24	1	16.24	0.47	0.5065	
	AC	35.28	1	35.28	1.01	0.3325	
	A^2	271.74	1	271.74	7.81	0.0152	
	Residual	452.59	13	34.81	452.59		
Uptake (mM/g)	Model	1.645E−004	6	2.741E−005	31.57	<0.0001	Significant
	A-RBB conc.	1.010E−004	1	1.010E−004	116.27	<0.0001	
	B-initial pH	7.036E−006	1	7.036E−006	8.10	0.0137	
	C-dosage	1.272E−005	1	1.272E−005	14.65	0.0021	
	AC	8.883E−008	1	8.883E−008	0.10	0.7542	
	BC	5.327E−007	1	5.327E−007	0.61	0.4475	
	A^2	4.315E−005	1	4.315E−005	49.69	<0.0001	
	Residual	1.129E−005	13	8.684E−007			

SS: sum of squares.
MS: mean square.
df: degrees of freedom.

Usually, the adequacy of the model can be confirmed by diagnostic plots, such as predicted vs. actual plots [25]. The amounts of R^2 for RBB removal and uptake models were 0.93 and 0.94, respectively, and also these amounts are in conformity with their "Adj R^2," which had 0.83 and 0.86, respectively.

3.3. Contour plots for RBB removal efficiency and uptake

Figs. 2 and 3 show the (2-D) two-dimensional response surfaces of RBB removal (%) and uptake. Fig. 2(a) shows the combined effect of initial pH and initial RBB concentration at constant initial MWCNTs concentration (250 mg). The graphs display that decrease in pH and RBB concentration has a positive effect on the overall dye removal efficiency. The maximum dye removal (73%) was observed for the concentration level of initial pH 5, initial RBB concentration 0.05 mM, and initial MWCVTs 250 mg.

The effect of initial dosage of MWCNTs and initial RBB concentration is shown in the Fig. 2(b). The maximum RBB of >68% was observed at the initial dosage 250 mg, 0.04 mM, and a constant initial pH 5.5. According to this figure, the amount of RBB removal

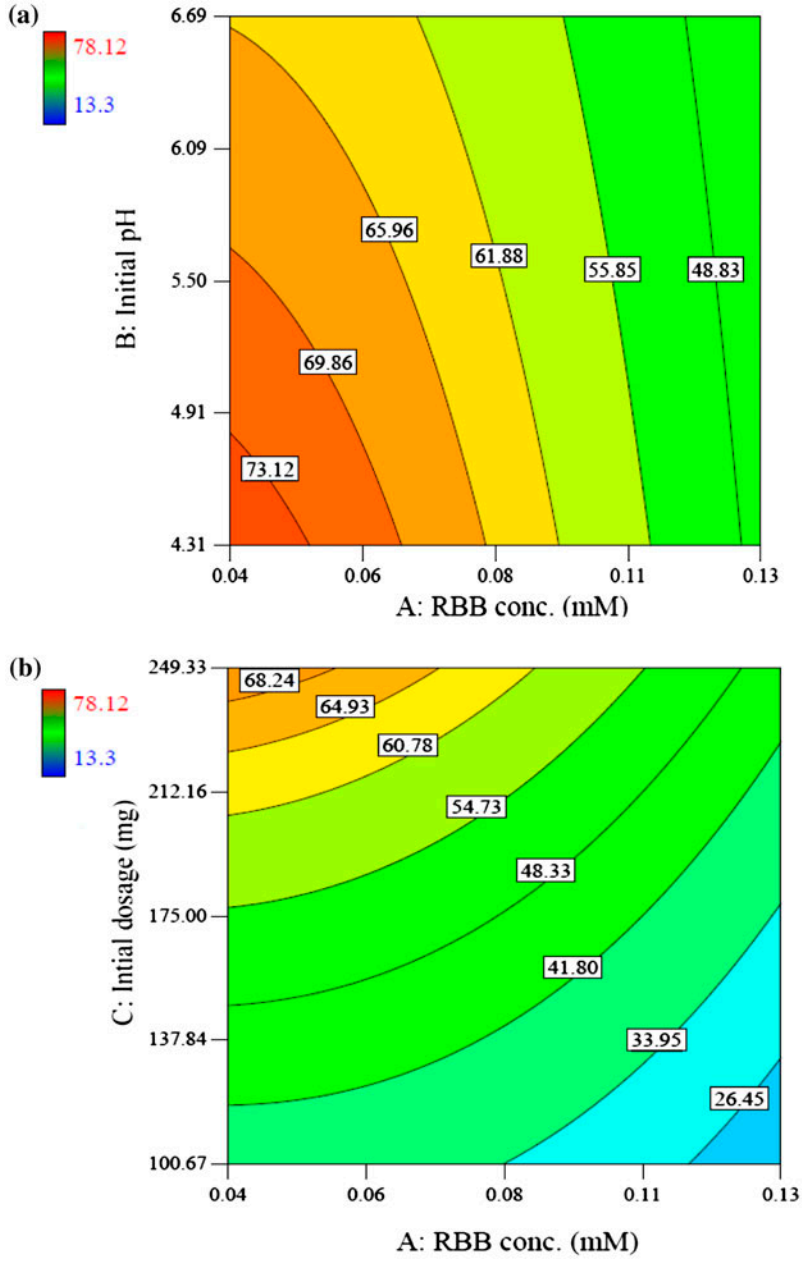

Fig. 2. Contour plot of response surface for RBB removal efficiency using MWCNTs, (a) interaction between the RBB concentration and initial pH at constant MWCNTs dosage of 250 mg and (b) interaction between the RBB concentration and initial dosage of MWCNTs at constant initial pH 5.5.

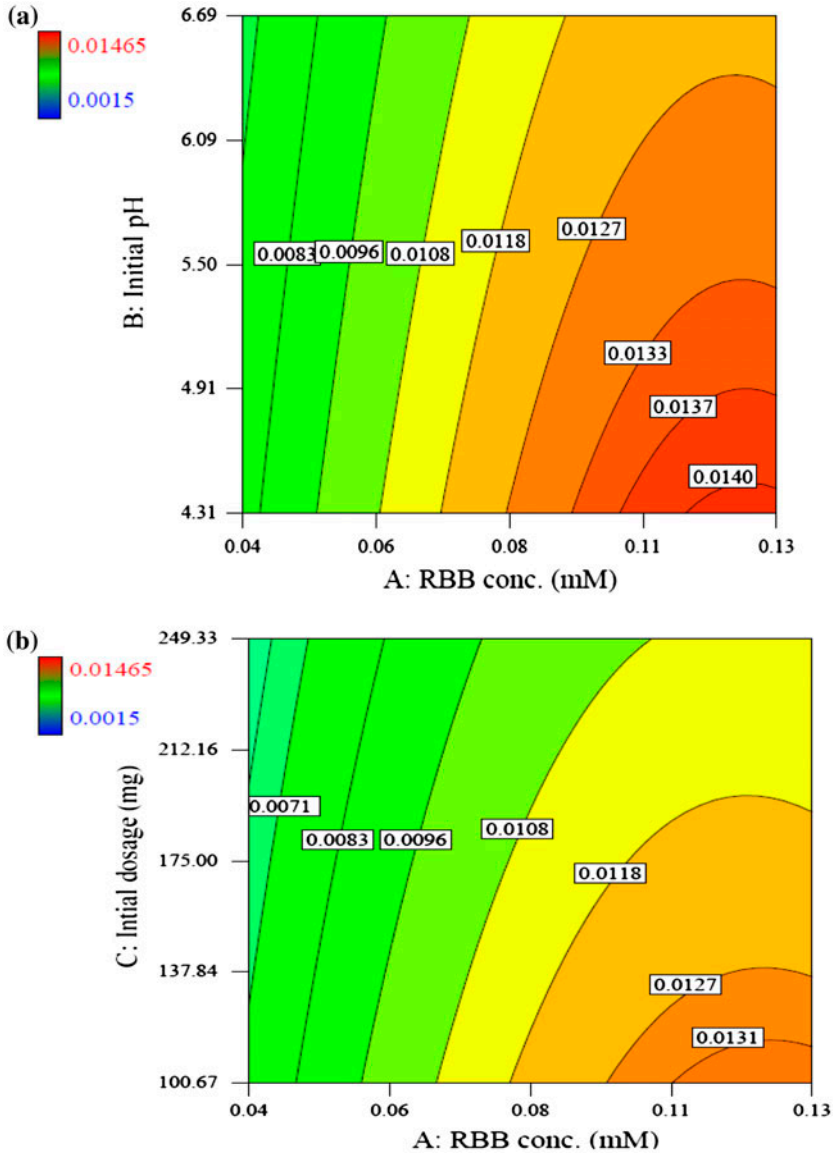

Fig. 3. Contour plot of response surface for dye uptake using MWCNTs, (a) interaction between the RBB concentration and initial pH at constant MWCNTs 100 and (b) interaction between the RBB concentration and initial dosage of MWCNTs at constant initial pH 5.5.

increased with initial RBB concentration, decreased from 0.13 to 0.04 mM, and initial dosage of MWCNTs increased from 100 to 250 mg. It is clear that the increase in MWCNTs dose results in an increase in the available surface area; therefore, the removal efficiency increased.

Fig. 3(a) shows the interaction between the initial pH and initial RBB concentration at the MWCNTs dosage 100 mg. RBB uptake increased with increase in initial RBB concentration from 0.04 to 0.13 mM and decrease in initial pH from 6.7 to 4.3. Fig. 3(b) indicates that the initial RBB concentration has a positive effect and the initial MWCNTs concentration has a negative effect on the RBB uptake. In the following, the effect of each factor was examined separately.

The adsorption capacity was expected to increase with increase in the inlet dye content because a high concentration difference provides a high driving force for the adsorption process [26]. This can occur mainly due to the increase in the mass transfer from the concentration gradient [27].

Decrease in initial pH due to the influence on the surface properties of the adsorbent and ionization/dissociation of the adsorbate molecule increased the

RBB uptake [28]. Depending on the pH of the dye solution, surface groups of MWCNTs change their valances and adsorption characteristics. At lower pH, more protons will be available to protonate amino groups of the adsorbent to form NH_3^+ groups, thereby increasing the electrostatic attractions between the negatively charged dye species and positively charged adsorption sites and causing an increase in the dye adsorption [29]. Also, the higher adsorption of the dye at lower pH is apparently due to greater accessibility of the dye to the active sites and more facile diffusion [30].

There is an increase in the RBB removal percentage with the increase in in MWCNTs dose due to more available surface area. In contrast to the removal percentage, with increase in the adsorbent dosage, adsorption capacity declined. This fact is due to the growing surface area and increase in the number of free sites available. When the adsorbent dosage increased, unsaturation of the active sites on the surface occurred and as a result, the adsorption capacity decreased [31]. But, loss in efficiency at higher adsorbent dose has been reported by Osorio et al., and it could be explained as a consequence of a partial aggregation of the adsorbent, which results in a decrease of the effective surface area for adsorbate uptake [32].

3.4. Process optimization using desirability functions

In the numerical optimization, a minimum and maximum level must be provided for each parameter. For several responses, the goals are combined into an overall desirability function [33]. Desirability is defined as an objective function that ranges from zero (0.00) outside of the limits to one (1.00) at the goal. The program seeks to maximize this function. By starting from several points in the design space, chances are highly improved for finding the best local maximum [34]. The maximum predicted RBB removal was 65.26% and RBB uptake was 0.0108 mM/g under optimal conditions of 0.086-mM RBB, 4.3 initial pH, and 250-mg MWCNTs dosage.

Numerical optimization under optimized conditions was used to test the validity and kinetics of the experiments, where multiple responses exist and regions where the requirements simultaneously meet the critical properties must be found. The best conciliation can be found visually by overlaying critical response contours on a contour plot. Fig. 4 is an overlay plot where the shaded portion (yellow color) indicates the zone of possible response values for the factor space and graphical optimization. The optimum

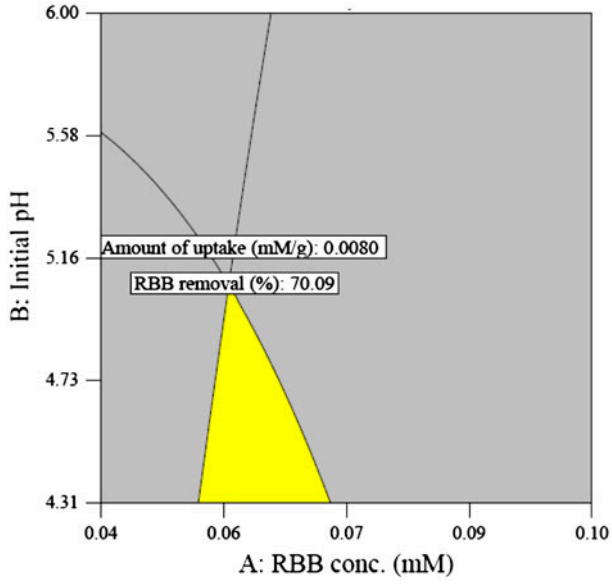

Fig. 4. Overlay plot.

region based on two critical responses was selected for RBB removal of 70% and RBB uptake of 0.008 mM/g.

3.5. Confirmatory experiment

To approve the validity of the optimized factors, an experiment was carried out with the parameters suggested by the model. Results predicted that values from fitted coefficient value were in close agreement at a 95% confidence interval. These results confirmed the validity of the model, and the experimental values were determined to be quite close to the predicted values. Under these conditions, the experimental value for the RBB removal and dye uptake was found to be 69.06% and 0.011 mM/g.

3.6. Isotherm studies

To analyze the adsorption equilibrium, the most three common isotherms including Langmuir, Freundlich, and Temkin models were evaluated. The linearized forms of equations were used for determining the equilibrium constants and coefficients. With regard to results, the maximum adsorption capacity (q_m), K_F, and B were determined. Coefficient value for the Langmuir, Freundlich and Temkin was 0.99, 0.87, and 0.95. Based on the coefficient value, the adsorption of the dye by carbon nanomaterials is best fitted with the Langmuir isotherm with $R^2 = 0.99$. The constant for the q_m and K_L was 0.02 (mM/g) and 382.8,

respectively. In the Langmuir isotherm, a single adsorbate binds to a single site on the adsorbent and all surface sites on the adsorbent have the same affinity for the adsorbate.

4. Conclusion

MWCNTs were used for the adsorption of RBB from aqueous solution. RSM was used to optimize the effective factors including initial pH, initial RBB concentration, and amount of MWCNTs dosage. Optimum values were initial pH 4.3, initial RBB concentration 0.08 mM, and amount of MWCNTs 250 mg. The maximum RBB removal and RBB uptake at the optimum condition was found 69.06% and 0.011 mM/g, respectively. Among the used isotherm models, the Langmuir isotherm was fitted with the experimental data, with high coefficient value (R^2 = 0.99).

References

[1] M.A. García-Morales, G. Roa-Morales, C. Barrera-Díaz, V. Martínez Miranda, P. Balderas Hernández, T.B. Pavón Silva, Integrated advanced oxidation process (ozonation) and electrocoagulation treatments for dye removal in denim effluents, Int. J. Electrochem. Sci. 8 (2013) 8752–8763.

[2] J. Mittal, D. Jharea, H. Vardhanb, A. Mittal, Utilization of bottom ash as a low-cost sorbent for the removal and recovery of a toxic halogen containing dye eosin yellow, Desalin. Water Treat. 52 (2014) 4508–4519.

[3] R. Gong, M. Li, C. Yang, Y. Sun, J. Chen, Removal of cationic dyes from aqueous solution by adsorption on peanut hull, J. Hazard. Mater. 121 (2005) 247–250.

[4] H. Daraei, A. Mittal, M. Noorisepehr, J. Mittal, Separation of chromium from water samples using eggshell powder as a low-cost sorbent: Kinetic and thermodynamic studies, Desalin. Water Treat. 52 (2015) 1307–1315.

[5] A. Ergene, K. Ada, S. Tan, H. Katırcıoğlu, Removal of Remazol Brilliant Blue R dye from aqueous solutions by adsorption onto immobilized *Scenedesmus quadricauda*: Equilibrium and kinetic modeling studies, Desalination 249 (2009) 1308–1314.

[6] T. Deveci, A. Unyayar, M.A. Mazmanci, Production of Remazol Brilliant Blue R decolourising oxygenase from the culture filtrate of *Funalia trogii* ATCC 200800, J. Mol. Catal. B-Enzym. 30 (2004) 25–32.

[7] I. Eichlerová, L. Homolka, O. Benada, O.K.T. Kofroňová, Tomáš Hubálek, Decolorization of Orange G and Remazol Brilliant Blue R by the white rot fungus *Dichomitus squalens*: Toxicological evaluation and morphological study, Chemosphere 69 (2007) 795–802.

[8] G. Moussavi, M. Mahmoudi, Degradation and biodegradability improvement of the reactive red 198 azo dye using catalytic ozonation with MgO nanocrystals, Chem. Eng. J. 152 (2009) 1–7.

[9] Y. Dong, K. He, B. Zhao, Y. Yin, L. Yin, A. Zhang, Catalytic ozonation of azo dye active brilliant red X-3B in water with natural mineral brucite, Catal. Commun. 8 (2007) 1599–1603.

[10] V.K. Gupta, A. Mittal, L. Krishnan, V. Gajbe, Adsorption kinetics and column operations for the removal and recovery of malachite green from wastewater using bottom ash, Sep. Purif. Technol. 40 (2004) 87–96.

[11] M.C. Wei, K.S. Wang, C.L. Huang, C.W. Chiang, T.J. Chang, S.S. Lee, S.H. Chang, Improvement of textile dye removal by electrocoagulation with low-cost steel wool cathode reactor, Chem. Eng. J. 192 (2012) 37–44.

[12] M. Koch, A. Yediler, D. Lienert, G. Insel, A. Kettrup, Ozonation of hydrolyzed azo dye reactive yellow 84 (CI), Chemosphere 46 (2002) 109–113.

[13] R. Maas, S. Chaudhari, Adsorption and biological decolourization of azo dye Reactive Red 2 in semicontinuous anaerobic reactors, Process. Biochem. 40 (2005) 699–705.

[14] P. Nigam, I.M. Banat, D. Singh, R. Marchant, Microbial process for the decolorization of textile effluent containing azo, diazo and reactive dyes, Process Biochem. 31 (1996) 435–442.

[15] A. Mittal, Adsorption kinetics of removal of a toxic dye, Malachite Green, from wastewater by using hen feathers, J. Hazard. Mater. 133 (2006) 196–202.

[16] A. Mittal, D. Jhare, J. Mittal, Adsorption of hazardous dye Eosin Yellow from aqueous solution onto waste material De-oiled Soya: Isotherm, kinetics and bulk removal, J. Mol. Liq. 179 (2013) 133–140.

[17] G. Nie, L. Zhang, Y. Cui, Preparation of Pd nanoparticles deposited on a polyaniline/multiwall carbon nanotubes nanocomposite and their application in the Heck reaction, React. Kinet. Mech. 108 (2013) 193–204.

[18] H. Hossini, A. Rezaee, S.O. Rastegar, S.E. Hashemi, M. Safari, Equilibrium and kinetic studies of chromium adsorption from wastewater by functionalized multi-wall carbon nanotubes, React. Kinet., Mech. Catal. 112 (2014) 371–382.

[19] V.K. Gupta, S. Agarwal, T.A. Saleh, Chromium removal by combining the magnetic properties of iron oxide with adsorption properties of carbon nanotubes, Water Res. 45 (2011) 2207–2212.

[20] E. Jiménez-Contreras, D. Torres-Salinas, R. Moreno, R. Ruiz Baños, E. Delgado López-Cózar, Response surface methodology and its application in evaluating scientific activity, Scientometrics 79 (2009) 201–218.

[21] R. Xiaoli, Y. Ling, L. Min, Kinetic and thermodynamic studies of acid scarlet 3R adsorption onto low-cost adsorbent developed from sludge and straw, Chin. J. Chem. Eng. 22 (2014) 208–213.

[22] L. Zhuannian, Z. Anning, W. Guirong, Z. Xiaoguang, Adsorption behavior of methyl orange onto modified ultrafine coal powder, Chin. J. Chem. Eng. 17 (2009) 942–948.

[23] M. Li, C. Feng, Z. Zhang, X. Liu, W. Ma, Q. Xue, N. Sugiura, Optimization of electrochemical ammonia removal using Box-Behnken design, J. Electroanal. Chem. 657 (2011) 66–73.

[24] M.J.K. Bashir, Application of response surface methodology (RSM) for optimization of ammoniacal nitrogen removal from semi-aerobic landfill leachate using ion exchange resin, Desalination 254 (2010) 154–161.

[25] M.H. Muhamad, S.R. Sheikh Abdullah, A.B. Mohamad, R. Abdul Rahman, A.A. Hasan Kadhum, Application of response surface methodology (RSM) for optimisation of COD, NH_3-N and 2,4-DCP removal from recycled paper wastewater in a pilot-scale granular activated carbon sequencing batch biofilm reactor (GAC-SBBR), J. Environ. Manage. 121 (2013) 179–190.
[26] A.A. Ahmad, B.H. Hameed, Fixed-bed adsorption of reactive azo dye onto granular activated carbon prepared from waste, J. Hazard. Mater. 175 (2010) 298–303.
[27] M.Ş. Tanyildizi, Modeling of adsorption isotherms and kinetics of reactive dye from aqueous solution by peanut hull, Chem. Eng. J. 168 (2011) 1234–1240.
[28] L. Wang, Application of activated carbon derived from 'waste' bamboo culms for the adsorption of azo disperse dye: Kinetic, equilibrium and thermodynamic studies, J. Environ. Manage. 102 (2012) 79–87.
[29] N.M. Mahmoodi, Dye removal from colored textile wastewater using chitosan in binary systems, Desalination 267 (2011) 64–72.
[30] V.K. Gupta, B. Gupta, A. Rastogi, S. Agarwal, A. Nayak, A comparative investigation on adsorption performances of mesoporous activated carbon prepared from waste rubber tire and activated carbon for a hazardous azo dye-Acid Blue 113, J. Hazard. Mater. 186 (2011) 891–901.
[31] T. Phuengprasop, J. Sittiwong, F. Unob, Removal of heavy metal ions by iron oxide coated sewage sludge, J. Hazard. Mater. 186 (2011) 502–507.
[32] A.G. Osorio, I.C.L. Silveira, V.L. Bueno, C.P. Bergmann, H_2SO_4/HNO_3/HCl-functionalization and its effect on dispersion of carbon nanotubes in aqueous media, Appl. Surf. Sci. 255 (2008) 2485–2489.
[33] M. Mourabet, A. El Rhilassi, H. El Boujaady, M. Bennani-Ziatni, R. El Hamri, A. Taitai, Removal of fluoride from aqueous solution by adsorption on hydroxyapatite (HAp) using response surface methodology, J. Saudi Chem. Soc., (2012). doi: 10.1016/j.jscs.2012.03.003.
[34] S.M.J. Mirazimi, F. Rashchi, M. Saba, Vanadium removal from roasted LD converter slag: Optimization of parameters by response surface methodology (RSM), Sep. Purif. Technol. 116 (2013) 175–183.